The MUC1 mucin protects against *Helicobacter pylori* pathogenesis in mice by regulation of the NLRP3 inflammasome

Short title: MUC1 regulation of the NLRP3 inflammasome

Garrett Z Ng[1,2], Trevelyan R Menheniott[2], Alison L Every[1], Andrew Stent[1], Louise M Judd[2], Yok Teng Chionh[1], Poshmaal Dhar[1, 2], Jasper C Komen[2], Andrew S Giraud[2], Timothy C Wang[3], Michael A McGuckin[4] and Philip Sutton[1,2#]

[1]Centre for Animal Biotechnology, School of Veterinary Science, University of Melbourne, Parkville, Victoria 3010, Australia

[2]Murdoch Childrens Research Institute, Royal Children's Hospital, Parkville, Victoria 3052, Australia

[3]Division of Digestive and Liver Diseases, Department of Medicine, Columbia University, New York, USA

[4]Mucosal Diseases Program, Mater Research Institute – University of Queensland, Translational Research Institute, Woolloongabba, Queensland 4102, Australia

[#]Correspondence: Associate Professor Philip Sutton, Mucosal Immunology, Murdoch Childrens Research Institute, Royal Children's Hospital, Parkville, Victoria 3052, Australia. phil.sutton@mcri.edu.au;
Ph: +61 3 9936 6751; Fax: +61 3 9936 6528

KEYWORDS: *Helicobacter pylori*; MUC1; IL-1β; inflammasome.

Word count = 4124

ABSTRACT

Objectives: The mucin MUC1, best known for providing an epithelial barrier, is an important protective host factor in both humans and mice during *Helicobacter pylori* pathogenesis. This study aimed to identify the long-term consequences of MUC1-deficiency on *H. pylori* pathogenesis and the mechanism by which MUC1 protects against *H. pylori* gastritis.

Design: Wildtype and *Muc1*$^{-/-}$ mice were infected for up to 9 months and the gastric pathology, immunological response and epigenetic changes assessed. The effects of MUC1 on the inflammasome, a potent inflammatory pathway, were examined in macrophages and *H. pylori* infected mice deficient in both MUC1 and inflammasome components.

Results: *Muc1*$^{-/-}$ mice began to die 6 months after challenge, indicating Muc1-deficiency made *H. pylori* a lethal infection. Surprisingly, chimaeric mouse infections revealed MUC1 expression by haematopoietic-derived immune cells limits *H. pylori*-induced gastritis. Gastritis in infected *Muc1*$^{-/-}$ mice was associated with elevated IL-1β and epigenetic changes in their gastric mucosa similar to those in transgenic mice over-expressing gastric IL-1β, implicating MUC1-regulation of an inflammasome. In support of this, infected *Muc1*$^{-/-}$*Casp1*$^{-/-}$ mice did not develop severe gastritis. Further, MUC1 regulated *Nlrp3* expression via an NF-κB-dependent pathway, and reduced NF-κB pathway activation via inhibition of IRAK4 phosphorylation. The importance of this regulation was proven using *Muc1*$^{-/-}$*Nlrp3*$^{-/-}$ mice which did not develop severe gastritis.

Conclusions: MUC1 is an important, previously unidentified negative regulator of the NLRP3 inflammasome. *H. pylori* activation of the NLRP3 inflammasome is normally tightly regulated by MUC1 and loss of this critical regulation results in the development of severe pathology.

SIGNIFICANCE OF THIS STUDY

What is already known on this topic

- *MUC1* polymorphisms are associated with gastric carcinogenesis in humans and MUC1 protects against *H. pylori* gastritis in mice
- MUC1 acts as a releasable decoy molecule to restrict bacterial adhesion to epithelial cells, thus preventing colonisation by *H. pylori*
- Polymorphisms in the IL-1β gene are also strongly associated with gastric carcinogenesis

What this study adds

- Experimental evidence that MUC1 is critical for survival of *H. pylori* infection
- MUC1 expression on immune cells, and not solely epithelial cells, limits gastritis during *H. pylori* infection
- MUC1 regulates NF-κB pathway activation to negatively regulate the NLRP3 inflammasome
- Regulation of NLRP3 inflammasome activity (by MUC1) is critical for the prevention of severe gastritis

How might it impact clinical practice in the foreseeable future?

- Dysregulation of the NLRP3 inflammasome may contribute to gastric carcinogenesis in certain individuals. Targeting the NLRP3 inflammasome may provide a potential approach for controlling gastric carcinogenesis

INTRODUCTION

A major constituent of the gastrointestinal surface are mucins, carbohydrate-rich glycoproteins that can be secreted or cell-surface associated, and which are best recognized for their protective role in mucosal barrier function. MUC1 is a cell-surface associated mucin, highly expressed on mucosal epithelial cells (and predominant on gastric epithelial cells) which provides an effective physical barrier against pathogens.[1, 2] Less well appreciated is that MUC1 is also expressed by immune cells, including B cells, T cells, monocytes, macrophages and dendritic cells.[3, 4, 5, 6] The potential role of MUC1 on these cells during mucosal infections is poorly understood.

H. pylori infection, typically acquired during childhood, is without treatment, normally present for the life of the host, resulting in a chronic gastritis that lasts for decades but with differing degrees of severity in different individuals infected with similar strains. In some individuals, typically those that develop severe gastritis, this constant inflammation induces, via stepwise progression, the development of gastric adenocarcinoma, the third most common cause of global cancer death.[7] Host factors that influence gastritis severity can have a major impact upon determining which *H. pylori*-infected individuals' progress to gastric cancer. The genetic factor most strongly associated with increased susceptibility to *H. pylori* associated diseases in many populations is the proinflammatory cytokine IL-1β.[8, 9, 10]

Human polymorphisms in *MUC1* are similarly associated with susceptibility to *Helicobacter*-associated gastritis and gastric adenocarcinoma, demonstrating a key role for MUC1 in regulating *H. pylori* related pathogenesis.[11, 12, 13] In mice, we have shown that MUC1 is a potent regulator of both *H. pylori* colonization and associated pathogenesis, with *Muc1*$^{-/-}$ mice developing an increased severity of *Helicobacter*-induced atrophic gastritis.[14] We identified that epithelial Muc1 regulates *H. pylori* colonization, by acting as a releasable decoy molecule that limits bacterial adhesion.[15] However, we now demonstrate that surprisingly, it is MUC1-expressing leukocytes which suppress *H. pylori*-induced gastritis, and that MUC1 mediates this protective effect by acting as a previously unrecognized negative regulator of the NLRP3 inflammasome.

MATERIALS AND METHODS

Mice

Specific-pathogen free *Muc1*$^{+/+}$ and *Muc1*$^{-/-}$ 129/Sv mice (kindly provided by Sandra Gendler)[16] were bred and housed in the Parkville Veterinary Science animal house, University of Melbourne. F3 *Muc1*$^{-/-}$*Casp1*$^{-/-}$, *Muc1*$^{-/-}$*Nlrp3*$^{-/-}$ and matched controls were generated by intercrossing *Muc1*$^{-/-}$ mice with *Casp1*$^{-/-}$ (*Casp11*-deficient)[17] or *Nlrp3*$^{-/-}$ C57BL/6 mice. For radiation chimeras, recipient mice were lethally irradiated with 2 doses of 550 rad three hours apart using a ^{60}Co source (Walter and Eliza Hall Institute of Medical Research) then, the next day, transplanted intravenously with 2×10^6 bone marrow cells harvested from the femurs and tibias of donor mice. Mice were maintained on drinking water containing 2 mg/mL neomycin (Gibco) for two weeks. Mice were left for two months prior to infection to allow reconstitution. All experiments were performed on age-matched female mice under University of Melbourne Animal Ethics Committee approval.

Bacterial culture and infection of mice

H. pylori SS1[18] was cultivated as described previously.[14] Mice were infected with a single oro-gastric dose of 10^7 *H. pylori* (estimated by light microscopy) suspended in 100 μL BHI.

Assessment of gastritis

Longitudinally halved stomachs were fixed in 10% neutral buffered formalin, embedded in paraffin and 5 μm sections stained with H&E. Infections were assessed histologically for infiltrating inflammatory immune cells, atrophy and dysplasia as previously described.[19, 20] For quantitatively assessing (gland) atrophy, 5 full glands were randomly selected from each of two images of corpus mucosa from blinded H&E or Alcian Blue/PAS stained sections. Using ImageJ, parietal cells were point counted.

Colony-forming assay and quantification of gastric cytokines by ELISA

Longitudinally halved stomachs were homogenised (T10 homogeniser, IKA-Werke) in BHI and colony-forming assay performed as described previously.[14] Culture supernatants and organ homogenates (homogenised in PBS or after colony-forming assay) were centrifuged to remove debris prior to quantification of cytokine by ELISA as previously described.[21] Primary antibodies: anti-mouse TNFα (0.1 μg/well; BioLegend), MIP-2 (0.1 μg/well; R&D Systems), IFNγ (0.1 μg/well; BD Biosciences), IL-17A (0.5 μg/well; eBioscience), IL-6 (0.05 μg/well; eBioscience), IL-1β (0.2 μg/well; R&D Systems), IL-10 (0.1 μg/well; BD

Biosciences), TGFβ (0.1 μg/well; BD Biosciences) or IL-18 (0.1 μg/well; R&D Systems). Secondary antibodies: biotinylated anti-mouse TNFα (0.025 μg/well), MIP-2 (3.7 ng/well), IFNγ (0.05 μg/well), IL-17A (0.025 μg/well), IL-6 (0.025 μg/well) IL-1β (0.03 μg/well), IL-10 (0.05 μg/well), TGFβ (0.05 μg/well) or IL-18 (1/2000; same manufacturers as capture antibody). Sample concentration was determined against a standard curve of recombinant cytokine (same manufacturers as antibodies).

Quantitative DNA methylation assays

Tff2 methylation levels were quantitated as described previously.[22] Briefly, genomic DNA (gDNA) was isolated from mouse stomach tissue using the DNeasy tissue kit (Qiagen) or using TriZOL (Invitrogen) and 500 ng was bisulphite-converted using Zymo EZ DNA methylation reagents (Zymo Research). Mouse *Tff2* fragments were recovered from bisulphite-converted gDNA by nested PCR. Quantitative methylation analysis of bisulphite PCR-amplified products was performed with the EPITYPER system (Sequenom Inc) using MassCLEAVE reagents followed by MALDI-TOF mass spectrometry. Data cleaning and 2-way hierarchical cluster analysis of methylation output values were performed using the R script and gplots software.

Flow cytometric analysis of inflammatory gastric cells

Gastric immune cells were isolated and stained as previously described,[21] using anti-MHCII-FITC (M5/114.15.2; Caltag Laboratories, Burlingame, CA), anti-Ly6C-PerCP (HK1.4; BioLegend), anti-CD64-PE (X54-5/7.1; BioLegend), anti-CD11c-PE.Cy5.5 (N418; eBioscience), anti-CD3-PE.Cy7 (145-2C11; BioLegend), anti-CD11b-Brilliant Violet 421 (M1/70; BioLegend), anti-CD19-Brilliant Violet 510 (6D5; BioLegend), anti-CD4-Brilliant Violet 650 (RM4-5; BioLegend), anti-CD103-Brilliant Violet 786 (2E7; BioLegend), anti-CD45-Alexa Fluor 700 (30-F11; eBioscience) and anti-Ly6G-APC.Cy7 (1A8; BioLegend). Cells were acquired on a BD Influx cell sorter (BD Biosciences), counts normalized using AccuCount Fluorescent Particles (Spherotech) and data analyzed using FCS Express. Gating strategies for innate cells were adapted from previous descriptions.[23, 24, 25]

Cell culture and stimulation

Non-induced peritoneal macrophages were isolated by flushing the peritoneal cavity with 10 mL of ice-cold PBS containing 2% (v/v) FCS (HyClone) and bone marrow-derived dendritic cells were cultured as described previously.[21] Cells were stimulated with *E. coli* LPS (100 ng/mL, Sigma), live *H. pylori* (MOI 10) or *H. pylori* sonicate lysate (5 μg/mL protein by BCA (Pierce)). To inhibit IKK activation, 12 μM BAY 11-7082 (Sigma) was added to cells for 45

min before stimulation. IRAK1/4 was inhibited by adding 1 μM IRAK1/4 Inhibitor I (Sigma) 30 min before stimulation. Stimulations were performed on 10^6 cells/mL in RPMI 1640 with 10% FCS, penicillin and streptomycin (Gibco).

Quantification of gene expression by qPCR

RNA was extracted using Tri Reagent (Ambion), then converted to cDNA using the Quantitect Reverse Transcription Kit (Qiagen). For long-term infected mice, RNA was extracted from paraffin embedded stomachs using the RNeasy FFPE Kit (Qiagen). For qPCR, duplicate reactions of 25 μL containing 12.5 μL QuantiTect SYBR Green PCR Master Mix (Qiagen), 0.2 μM primers and 3 μL of cDNA (diluted to 150μL) were performed in an Mx3000P cycler (Stratagene). Primer efficiencies were calculated with LinRegPCR,[26] and relative expression calculated relative to *Actb*. Primers: *Actb* – F, 5'-CGTGAAAAGATGACCCAGATCA-3', R, 5'-CACAGCCTGGATGGCTACGT-3'; *Nlrp3* – F, 5'-ATGGTATGCCAGGAGGACAG-3', R, 5'-ATGCTCCTTGACCAGTTGGA-3'; *Tff2* – F, 5'-CCCCACAACAGAAAGAAC-3', R, 5'-GGGCACTTCAAAGATCAG-3'.

Western blotting

Cell lysates were collected in radioimmunoprecipitation buffer (150 mmol/L NaCl, 1% IGEPAL, 0.5% deoxycholic acid, 0.1% SDS, 50 mmol/L Tris, pH 7.5) containing protease inhibitor cocktail (Complete, mini, EDTA-free; Roche). Samples were separated on 8% SDS-PAGE gels then transferred to nitrocellulose membranes (Amersham Biosciences). Membranes were blocked with 5% skim milk and probed with anti-NLRP3 antibody (Cryo-2; Adipogen), anti-phospho-p65, anti-total p65, anti-phospho-IKKα/β, anti-IKKβ, anti-phospho-IRAK4, anti-total IRAK4 or anti-β-actin (all from Cell Signaling). Bound primary antibodies were detected with HRP-conjugated anti-rabbit (Dako). Labelled proteins were visualized by incubating the membrane in ECL Prime reagent (Amersham Biosciences) and using an ImageQuant LAS 4000 (GE Healthcare). Sodium fluoride was added to radioimmunoprecipitation buffer and skim milk at 20 mM or to other buffers at 2 mM when assessing phosphorylation. Densitometry was performed using ImageJ.

Statistics

Survival was assessed using the Mantel-Cox test. Nonparametric histological gradings were analysed using Mann-Whitney U tests to assess relative severity and Fisher's exact test to assess absence or presence of criteria. All other data were analysed using one-way ANOVAs with Dunnett's post-hoc test.

RESULTS

High mortality and gastric dysplasia in long-term *H. pylori*-infected *Muc1*$^{-/-}$ mice

Previous studies demonstrated a dramatic increase in gastritis severity in *Muc1*$^{-/-}$ mice infected with *H. pylori* for 2 months.[14, 27] To examine the role of MUC1 during the life-long chronic infection typical of *H. pylori*, mice were infected and left long-term. While uninfected control and infected wildtype mice remained asymptomatic throughout the study, infected *Muc1*$^{-/-}$ mice progressively developed clinical signs of disease (including ruffled fur, hunched posture and inactivity) from approximately 200 days post-infection, which necessitated euthanasia due to ethical considerations. Overall, *H. pylori*-infected *Muc1*$^{-/-}$ mice had a highly significant increase in mortality, with a median survival of 284 days after infection (Fig. 1A). High mortality in infected *Muc1*$^{-/-}$ mice was associated with an increased mononuclear cell infiltrate and severity of atrophic gastritis (Fig. 1B). Most notably, Muc1 expression significantly protected against development of the precancerous lesion, gastric dysplasia, following long-term *H. pylori* infection. The incidence of dysplasia was 94% in infected *Muc1*$^{-/-}$ mice versus 59% in infected wildtype mice (Fig. 1B; p=0.011, Fisher's exact test). Representative photomicrographs of the gastric mucosa are shown in Fig. 2, with an increase in transmural inflammatory infiltrate, atrophy and dysplasia being evident in the infected cohorts. We characterised the dysplastic cells in infected *Muc1*$^{-/-}$ mice and found that the majority of cells stain for both acidic and neutral carbohydrates (Alcian Blue/PAS) (Fig. S1). In addition, dysplastic cells also stained with UEA-I, and weakly for TFF2, but not GS-II suggesting that they were derived from surface mucous cell lineage (Fig. S1). Contrary to two months post-infection,[14] long-term infected *Muc1*$^{-/-}$ mice had less bacterial colonisation (Fig. 1C), likely due to the extremely severe pathology resulting in the gastric environment becoming less hospitable to colonisation. This is consistent with most other models of *H. pylori* infection [28, 29].

Severe pathology in *Muc1*$^{-/-}$ mice is associated with elevated IL-1β, hypermethylation and silencing of *Tff2*

To characterize the accentuated *H. pylori*-induced gastritis observed in MUC1-deficiency, we assessed key cytokines in the gastric tissues of mice infected for 1, 2 or 8 months. No difference was observed in proinflammatory TNFα, IL-6, MIP-2, IFNγ or IL-17A in stomachs from uninfected and *H. pylori* infected wildtype and *Muc1*$^{-/-}$ mice at any time-point (Fig. 3A-E). Notably, IL-1β was the only measured proinflammatory cytokine significantly elevated in *H. pylori* infected *Muc1*$^{-/-}$ mice (Fig. 3F). IL-1β levels increased at two months post-infection,

coinciding with development of atrophic gastritis in these animals.[14] Hence in wildtype mice, reduced IL-1β production paralleled reduced inflammation. We also assessed the immunoregulatory cytokines IL-10 and TGFβ. Although no difference was observed in IL-10, *Muc1*$^{-/-}$ mice had significantly elevated TGFβ after two months of infection (Fig. 3G, H), which likely represents an attempt to regulate inflammation in these animals.

Previous experiments revealed that stomach-specific overexpression of human IL-1β in mice leads to gastritis, dysplasia and cancer in the absence of *H. pylori* infection.[30] We have reported previously that Trefoil factor 2 (TFF2)-deficient mice also display accelerated progression from gastritis to dysplasia after infection with *H. pylori*.[31] TFF2, a member of the trefoil factor family of secreted peptides, has well-established roles in the maintenance of gastric epithelial homeostasis.[22, 32] Additionally, loss of *TFF2* expression via methylation of promoter and first exon sites (as indicated in Fig. 4A) is a pivotal epigenetic event underlying gastric tumorigenesis in humans and mice.[22] We hypothesized that elevated IL-1β expression alone is sufficient to induce *Tff2* epigenetic silencing. Consistent with this, *Tff2* mRNA levels were substantially reduced in stomachs of IL-1β transgenic (IL-1β^{Tg}) mice compared to wildtype littermate controls (Fig. 4B), while methylation was increased (Fig. 4C, D).

Given this observation and that the phenotype of *Muc1*$^{-/-}$ mice infected long-term with *H. pylori* bore a striking resemblance to that of *Tff2*$^{-/-}$ mice, we hypothesized that epigenetic silencing leading to loss of *Tff2* expression could be an underlying mechanism for severe gastric pathology in *H. pylori*-infected *Muc1*$^{-/-}$ mice. At 2 months post-infection there was a non-significant increase in *Tff2* methylation in *Muc1*$^{-/-}$ mice (data not shown). By contrast, analysis after long-term infection revealed elevated *Tff2* methylation in *H. pylori*-infected mice, with infected *Muc1*$^{-/-}$ mice presenting significantly elevated *Tff2* methylation compared to infected wildtype controls (Fig. 4E). Differences in *Tff2* methylation after long-term infection allowed *H. pylori*-infected *Muc1*$^{-/-}$ mice to be broadly distinguished from uninfected and infected wildtype controls in two-way hierarchical clustering analysis (Fig. 4F). Therefore, aberrant *Tff2* methylation was acquired in concert with the progression of gastric pathology in *Muc1*$^{-/-}$ mice. Both long-term infected wildtype and *Muc1*$^{-/-}$ mice had clearly reduced expression of *Tff2* mRNA (Fig. 4G), suggesting that even the intermediate *Tff2* methylation observed in infected wildtype mice was capable of reducing *Tff2* expression.

These results are consistent with the hypothesis that IL-1β promotes pre-neoplastic progression in *Muc1*$^{-/-}$ mice, at least in part, by inducing methylation and silencing of *Tff2*.

Severe *H. pylori* gastritis results from MUC1-deficiency on haematopoietic-derived cells and is caspase-1-dependent

Radiation chimaeras were used to assess the relative contributions of MUC1-expressing haematopoietic and non-haematopoietic cells in regulating *H. pylori*-induced gastritis. Only mice lacking haematopoietic MUC1 developed significant atrophic gastritis, and this occurred regardless of their non-haematopoietic genotype (Fig. 5). Thus, it was MUC1 expressed on immune cells (and not epithelial cells) that regulated the severity of *H. pylori*-induced gastritis.

Phenotyping the main types of immune cells present in the stomachs of infected mice by flow cytometry (gating strategy shown in Fig. 6A) revealed no differences in the absolute numbers of T cells, a trend towards increased monocyte/macrophages, B cells and neutrophils, and significantly increased numbers of dendritic cells (Fig. 6B). Further analysis of the monocyte/macrophage population revealed that specifically the P2 subset, which has elevated inflammatory activity,[24] was significantly increased in *Muc1*$^{-/-}$ mice (Fig. 6B). One population of cells we have previously shown were recruited by elevated IL-1b are myeloid-derived suppressor cells (MDSCs).[30] To see whether there was preferential recruitment of these cells in *Muc1*$^{-/-}$ mice, we assessed CD11b+Ly6G/Ly6C+ cells and expression of *S100a8/S100a9*, proinflammatory chemokines that correlate with MDSC presence. While infection increased both types of myeloid cells and *S100a8/S100a9* expression, there was no difference between wildtype and *Muc1*$^{-/-}$ mice (Fig. S2).

The association between elevated IL-1β and severe *H. pylori* gastritis indicated Muc1 may regulate inflammasome(s), multimeric proteolytic complexes responsible for processing inactive pro-IL-1β and pro-IL-18 into mature cytokines. Stimulation of both macrophages and dendritic cells, cells commonly used to examine inflammasome activation and IL-1β production, with either live *H. pylori* or bacterial lysate induced IL-1β secretion (Fig. 7A). Glyburide (an NLRP3 inflammasome inhibitor) significantly reduced the levels of IL-1β (Fig. 7A), demonstrating that IL-1β production was at least in part dependent on the NLRP3 inflammasome. Assessment of *Muc1*$^{-/-}$ cells revealed macrophages but not dendritic cells, produced significantly increased IL-1β compared to wildtype cells in response to *H. pylori* lysate (Fig. 7B). *Muc1*$^{-/-}$ macrophages also produced significantly elevated levels of IL-18 (Fig. 7C).

As caspase-1 is the main effector protease responsible for inflammasome activity, we generated mice deficient in both *Muc1* and *Casp1*. When infected with *H. pylori*, *Muc1*$^{-/-}$ but not matched *Muc1*$^{-/-}$*Casp1*$^{-/-}$ mice developed significant atrophic gastritis (Fig. 7D, E),

indicating that severe pathology in infected *Muc1*$^{-/-}$ mice was the result of increased inflammasome activation.

MUC1 regulates expression of NLRP3

While several distinct inflammasome complexes exist, *H. pylori* has been previously shown capable of activating the NLRP3 inflammasome.[33, 34] We found that *Nlrp3* expression was significantly increased in the stomachs of *Muc1*$^{-/-}$ but not wildtype mice infected with *H. pylori* for two months (Fig. 8A). Further, western blotting showed that *Muc1*$^{-/-}$ macrophages had significantly increased NLRP3 protein levels compared to wildtype cells after 3 hours of LPS or *H. pylori* lysate stimulation (Fig. 8B), indicating MUC1 regulates NLRP3 expression following TLR activation.

As human MUC1 is known to regulate the NF-κB pathway,[35, 36, 37] and activation of this pathway can regulate NLRP3 expression,[38] we hypothesized that MUC1 may inhibit NLRP3 inflammasome activation by negative regulation of TLR signalling. Treatment with the IKK inhibitor BAY 11-7082, prior to LPS or *H. pylori* lysate stimulation, completely inhibited *Nlrp3* upregulation in both wildtype and *Muc1*$^{-/-}$ macrophages (Fig. 8C), indicating that the increased *Nlrp3* expression was indeed dependent on activation of NF-κB and not other transcription factors activated by TLRs, including AP-1.[39] We also assessed i) miR-223 levels, as this regulates *Nlrp3* expression,[40] and ii) the ATP-synthesizing capacity of macrophages as an indirect measure of mitochondrial membrane perturbation, which is intimately linked with NLRP3 activation,[41] but found no effect of MUC1 on either measure (Fig. S3, S4).

We next examined several key intermediates along the TLR/NF-κB pathways to determine where murine MUC1 regulated NF-κB activation. Western blotting revealed that phosphorylation and activation of p65 was accentuated in *Muc1*$^{-/-}$ macrophages after LPS or *H. pylori* lysate treatment (Fig. 8D, E). An interaction between human MUC1 oncoprotein and IKKs, the initial kinases of the NF-κB pathway upstream of p65, has previously been suggested,[42] and we noted that *Muc1*$^{-/-}$ cells displayed increased IKKα/β activity after LPS stimulation (Fig. 8D). We finally examined activation of IRAK4, the first kinase activated in the TLR pathway. Importantly, we found significantly increased activation of IRAK4 in *Muc1*$^{-/-}$ macrophages following stimulation with either LPS (Fig. 8F), or *H. pylori* lysate (Fig. 8G). We confirmed that *Nlrp3* upregulation in response to *H. pylori* lysate was indeed dependent on IRAK4 activation by treatment with IRAK1/4 inhibitor, which abrogated upregulation of *Nlrp3* (Fig. 8H).

This indicates that Muc1 regulates NF-κB activation by suppressing the initial steps of TLR activation. The increased NLRP3 inflammasome activity in *Muc1*$^{-/-}$ cells therefore results from increased expression of NLRP3 due to a loss of regulation of the TLR/NF-κB pathways at or above the level of IRAK4.

Atrophic gastritis in *Muc1*$^{-/-}$ mice is Nlrp3-dependent

To examine the role of the NLRP3 inflammasome in the severe gastritis observed in *H. pylori* infected *Muc1*$^{-/-}$ mice, we generated mice deficient in both *Muc1*$^{-/-}$ and *Nlrp3*$^{-/-}$. *Muc1*$^{-/-}$ but not *Muc1*$^{-/-}$*Nlrp3*$^{-/-}$ macrophages produced significantly more IL-1β in response to *H. pylori* lysate (Fig. 9A). Infected *Muc1*$^{-/-}$, but not *Muc1*$^{-/-}$*Nlrp3*$^{-/-}$ mice had a significant increase in gastric IL-1β and IL-18 levels (Fig. 9B). In addition, only infected *Muc1*$^{-/-}$ mice developed a significant atrophic gastritis (Fig. 9C, D). This demonstrates that the severe *H. pylori*-induced gastritis and elevated IL-1β levels observed in *Muc1*$^{-/-}$ mice resulted from a loss of regulation of the NLRP3 inflammasome that is activated by *H. pylori* infection.

DISCUSSION

Excessive or misdirected inflammation is a central aspect of many gastrointestinal diseases, and thus regulatory mechanisms that limit immune over-activation are of great importance. The NLRP3 inflammasome is activated by a large array of ligands and therefore the potential for harmful non-specific activation is much greater than for other innate receptors. Here we show that the cell-associated mucin MUC1 plays a key role in negatively regulating NLRP3 inflammasome activity on immune cells, ultimately restraining the inflammation induced by chronic *H. pylori* infection. Further, we demonstrate that this occurs via the ability of MUC1 to regulate NLRP3 expression via suppression of TLR/NF-κB pathway activation. Profound effects on mortality, dysplasia and epigenetic changes demonstrate the functional importance of MUC1 regulation of NLRP3 inflammasome activation.

MUC1 was first linked with increased susceptibility to *H. pylori* related pathologies more than a decade ago,[11, 12] although the mechanism behind this observation remains unclear. Consistent with the prevailing understanding of the role of MUC1, we previously proposed that elevated gastritis in *Muc1*$^{-/-}$ mice could be due to the ability of MUC1 to limit pathogen contact with the host epithelium.[14, 15] However, our latest findings surprisingly indicate that leukocyte MUC1 directly regulates the host immune system to limit activation of the NLRP3 inflammasome.

Regarding *H. pylori*, both TLR2 and NOD2 activation induce expression of NLRP3, which then acts as the primary inflammasome activator to bacterial virulence factors including the *cag* pathogenicity island (*cag*PAI) and VacA.[33, 34] In our experiments the SS1 strain, which possesses a dysfunctional *cag*PAI,[43] was used indicating that *cag*PAI-independent NLRP3 activation must also occur. Here we show that increased NLRP3 expression occurs in the absence of MUC1, in conjunction with increased phosphorylation of IRAK4, IKKs and p65, indicating MUC1 limits NLRP3 activation by suppression of TLR/NF-κB-dependent priming. Our demonstration here of the regulatory role of MUC1 is, to our knowledge, the first to clearly establish the importance of NF-κB regulation in preventing excessive NLRP3 inflammasome activation, as evidenced by the severe pathology and mortality observed in infected *Muc1*$^{-/-}$ mice.

In support of our findings, previous studies have shown that MUC1 negatively regulates TLR signalling and subsequent NF-κB activation,[35, 36, 37] although the precise mechanism for this effect was not identified. We now demonstrate for the first time that MUC1 negatively regulates phosphorylation of IRAK4. During TLR activation, IRAK4 is recruited to the cell membrane where it binds to TLR cytoplasmic domains via MyD88, well upstream of IKK activation.[44] This demonstrates that MUC1 influences TLR/NF-κB signalling at a much earlier point than shown previously, potentially via direct interactions with TLRs, MyD88 or IRAK4, which all localize at the cell membrane during TLR activation. MUC1 has previously been demonstrated to directly associate with TLR5 and inhibit MyD88 binding,[45] thus further supporting a role for MUC1 in regulating the initial stages of TLR activation.

Another surprising finding was the lack of increase in proinflammatory cytokines assessed other than IL-1β within the inflamed gastric mucosa of infected *Muc1*$^{-/-}$ or 129/SvJ mice. We believe the specific cytokine profile is due to the 129/SvJ genetic background, which could have aided our investigation into the modulation of IL-1β by MUC1. A key difference between 129 strains, such as the 129/SvJs used in our studies, from mice used in other studies is defective caspase-11.[17] Another contributing factor may have been MDSCs, which are well known to have potent immunosuppressive ability and are recruited following elevated gastric IL-1β.[30] However, our data suggest MDSCs were recruited into the *H. pylori* infected stomachs of both wildtype and *Muc1*$^{-/-}$ 129/Sv mice, even though only the *Muc1*$^{-/-}$ mice had elevated gastric IL-1β. As such cells could suppress secretion of other cytokines, this recruitment may explain the unusually specific cytokine profile observed after infection in 129/Sv mice, although the mechanism of MDSC recruitment does not appear to involve IL-1β.

Recent studies in mice have demonstrated that during *Helicobacter* infection, IL-1β promotes atrophic gastritis and neoplasia while IL-18 limits gastritis through promoting regulatory T cell development,[30, 46, 47] demonstrating that inflammasome activation in the host can contribute both pro and anti-inflammatory activity. Overall, NLRP3 inflammasome activity is proinflammatory *in vivo*, with *Nlrp3*$^{-/-}$ mice displaying reduced gastritis after infection.[34] An important observation that emerges with the use of *Muc1*$^{-/-}$ mice is that *H. pylori* is a potent activator of the NLRP3 inflammasome, but under normal circumstances this is not overtly apparent, due to host regulation of this process. This is consistent with the only minor reduction in gastritis observed after *H. pylori* infection of *Asc*$^{-/-}$ mice, which should lack all inflammasome activity.[48] Full activation of the NLRP3 inflammasome probably only develops when regulation is lost, for example in the absence of MUC1. Under those conditions, the consequences are clearly severe as *H. pylori*, normally a fairly benign colonizer of conventional mice, became a lethal infection with the development of gastric dysplasia.

Although a causative role of aberrant inflammation on tumorigenesis is now accepted, exactly how innate inflammatory molecules such as IL-1β drive gastric tumorigenesis remains unclear. We have previously demonstrated the causative role of i) elevated IL-1β and ii) silencing of *Tff2* individually in gastric tumorigenesis.[22, 30, 31] In this study we demonstrate a potential link between these factors showing that gastric IL-1β overexpression in both transgenic mice and in *H. pylori* infected *Muc1*$^{-/-}$ mice is associated with *Tff2* methylation. IL-1β has previously been described to promote the activity of DNA methyltransferase-1 via nitric oxide production, resulting in aberrant methylation of *FMR1* and *HPRT*.[49] While only *Tff2* has been studied, it is possible that a spectrum of other genes, including tumour suppressor genes, are similarly affected. Regardless of *Tff2*, this provides a framework to explain how inflammatory molecules (and modulators such as MUC1) may promote tumorigenesis, and potentially provides a clinical approach via the targeting of IL-1β or the NLRP3 inflammasome.

In summary, we have demonstrated that MUC1 on immune cells is a novel regulator of the NLRP3 inflammasome, and propose this is mediated by an interaction with signalling components at the cytoplasmic domains of TLRs that involves inhibition of IRAK4 activation. In the absence of appropriate regulation, the NLRP3 inflammasome is a key driver of *H. pylori*-induced pathologies via the promotion of gastric IL-1β production, which we propose leads to epigenetic silencing of tumour suppressor gene expression and is associated with the development of gastric dysplasia. Hence while mucins are currently best recognized

for key roles at epithelial surfaces, MUC1 clearly also plays a fundamentally important and previously unidentified role in regulating the response of immune cells to certain inflammatory stimuli.

ACKNOWLEDGEMENTS

The authors thank Ben Croker for providing *Casp1*$^{-/-}$ and *Nlrp3*$^{-/-}$ mice.

Contributors: PS and MAM obtained funding. GZN, TRM, ALE, ASG, MAM and PS designed and analysed experiments. GZN, TRM, ALE, AS, YTC, PD and JCK performed the experiments. GZN and LMJ performed histological analyses. TCW provided IL-1^{Tg} mice. GZN, TRM and PS prepared the manuscript. All authors revised and approved the final manuscript.

Competing interests: The authors have no conflicts to declare.

Funding: This work was supported by the Victorian Government's Operational Infrastructure Support Program and by Project Grant #1046254 from the National Health and Medical Research Council of Australia. PS and MAM are supported by Senior Research Fellowships from the NHMRC and GZN was partly supported by a Melbourne Research Scholarship from The University of Melbourne.

REFERENCES

1 Lindén SK, Sutton P, Karlsson NG, et al. Mucins in the mucosal barrier to infection. *Mucosal Immunol* 2008;**1**:183-97.

2 McGuckin MA, Lindén SK, Sutton P, et al. Mucin dynamics and enteric pathogens. *Nat Rev Micro* 2011;**9**:265-78.

3 Brugger W, Buhring H-J, Grunebach F, et al. Expression of MUC-1 epitopes on normal bone marrow: implications for the detection of micrometastatic tumor cells. *J Clin Oncol* 1999;**17**:1535-44.

4 Agrawal B, Krantz MJ, Parker J, et al. Expression of MUC1 mucin on activated human T cells: implications for a role of MUC1 in normal immune regulation. *Cancer Res* 1998;**58**:4079-81.

5 Leong C, Raudhawati O, Cheong S, et al. Epithelial membrane antigen (EMA) or MUC1 expression on monocytes and monoblasts. *Pathology* 2003;**35**:422-7.

6 Wykes M, MacDonald KPA, Tran M, et al. MUC1 epithelial mucin (CD227) is expressed by activated dendritic cells. *J Leukoc Biol* 2002;**72**:692-701.

7 International Agency for Research on Cancer. GLOBOCON 2012: Estimated cancer incidence, mortality and prevalence worldwide in 2012. . *World Health Organization* 2012.

8 El-Omar EM, Carrington M, Wong-Ho C, et al. Interleukin-1 polymorphisms associated with increased risk of gastric cancer. *Nature* 2000;**404**:398-402.

9 Rad R, Prinz C, Neu B, et al. Synergistic effect of *Helicobacter pylori* virulence factors and interleukin-1 polymorphisms for the development of severe histological changes in the gastric mucosa. *J infect Dis* 2003;**188**:272-81.

10 Kato S, Onda M, Yamada S, et al. Association of the interleukin-1β genetic polymorphism and gastric cancer risk in Japanese. *J Gastroenterol* 2001;**36**:696-9.

11 Vinall LE, King M, Novelli M, et al. Altered expression and allelic association of the hypervariable membrane mucin MUC1 in *Helicobacter pylori* gastritis. *Gastroenterology* 2002;**123**:41.

12 Carvalho F, Seruca R, David L, et al. MUC1 gene polymorphism and gastric cancer - an epidemiological study. *Glycoconjugate J* 1997;**14**:107.

13 Saeki N, Saito A, Choi IJ, et al. A functional single nucleotide polymorphism in Mucin 1, at chromosome 1q22, determines susceptibility to diffuse-type gastric cancer. *Gastroenterology* 2011;**140**:892-902.

14 McGuckin MA, Every AL, Skene CD, et al. Muc1 mucin limits both *Helicobacter pylori* colonization of the murine gastric mucosa and associated gastritis. *Gastroenterology* 2007;**133**:1210-8.

15 Lindén SK, Sheng YH, Every AL, et al. MUC1 limits *Helicobacter pylori* infection both by steric hindrance and by acting as a releasable decoy. *PLoS Pathog* 2009;**5**:e1000617.

16 Spicer AP, Rowse GJ, Lidner TK, et al. Delayed mammary tumor progression in Muc-1 null mice. *J Biol Chem* 1995;**270**:30093-101.

17 Kayagaki N, Warming S, Lamkanfi M, et al. Non-canonical inflammasome activation targets caspase-11. *Nature* 2011;**479**:117-21.

18 Lee A, O'Rourke J, De Ungria MC, et al. A standardized mouse model of *Helicobacter pylori* infection: introducing the Sydney strain. *Gastroenterology* 1997;**112**:1386-97.

19 Sutton P, Danon SJ, Walker M, et al. Post-immunisation gastritis and *Helicobacter* infection in the mouse: a long term study. *Gut* 2001;**49**:467-73.

20 Howlett M, Judd LM, Jenkins B, et al. Differential regulation of gastric tumor growth by cytokines that signal exclusively through the coreceptor gp130. *Gastroenterology* 2005;**129**:1005-18.

21 Chionh YT, Ng GZ, Ong L, et al. Protease-activated receptor 1 suppresses *Helicobacter pylori* gastritis via the inhibition of macrophage cytokine secretion and interferon regulatory factor 5. *Mucosal Immunol* 2015;**8**:68-79.

22 Peterson AJ, Menheniott TR, O'Connor L, et al. *Helicobacter pylori* infection promotes methylation and silencing of trefoil factor 2, leading to gastric tumor development in mice and humans. *Gastroenterology* 2010;**139**:2005-17.

23 Quiding-Järbrink M, Raghavan S, Sundquist M. Enhanced M1 macrophage polarization in human Helicobacter pylori-associated atrophic gastritis and in vaccinated mice. *PLoS One* 2010;**5**:e15018.

24 Bain CC, Scott CL, Uronen-Hansson H, et al. Resident and pro-inflammatory macrophages in the colon represent alternative context-dependent fates of the same Ly6C^{hi} monocyte precursors. *Mucosal Immunol* 2013;**6**:498-510.

25 Tamoutounour S, Henri S, Lelouard H, et al. CD64 distinguishes macrophages from dendritic cells in the gut and reveals the Th1-inducing role of mesenteric lymph node macrophages during colitis. *European Journal of Immunology* 2012;**42**:3150-66.

26 Ramakers C, Ruijter JM, Deprez RHL, et al. Assumption-free analysis of quantitative real-time polymerase chain reaction (PCR) data. *Neurosci Lett* 2003;**339**:62-6.

27 Every AL, Ng GZ, Skene CD, et al. Localized suppression of inflammation at sites of *Helicobacter pylori* colonization. *Infect Immun* 2011;**79**:4186-92.

28 Eaton KA, Mefford M, Thevenot T. The role of T Cell cubsets and cytokines in the pathogenesis of *Helicobacter pylori* gastritis in mice. *J Immunol* 2001;**166**:7456-61.

29 Wee JLK, Chionh YT, Ng GZ, et al. Protease-activated receptor-1 down-regulates the murine inflammatory and humoral response to Helicobacter pylori. *Gastroenterology* 2010;**138**:573-82.

30 Tu S, Bhagat G, Cui G, et al. Overexpression of interleukin-1β induces gastric inflammation and cancer and mobilizes myeloid-derived suppressor cells in mice. *Cancer Cell* 2008;**14**:408-19.

31 Fox JG, Rogers AB, Whary MT, et al. Accelerated progression of gastritis to dysplasia in the pyloric antrum of TFF2$^{-/-}$ C57BL6 × Sv129 *Helicobacter pylori*-infected mice. *Am J Pathol* 2007;**171**:1520-8.

32 Farrell JJ, Taupin D, Koh TJ, et al. TFF2/SP-deficient mice show decreased gastric proliferation, increased acid secretion, and increased susceptibility to NSAID injury. *J Clin Invest* 2002;**109**:193-204.

33 Kim DJ, Park JH, Franchi L, et al. The Cag pathogenicity island and interaction between TLR2/NOD2 and NLRP3 regulate IL-1beta production in *Helicobacter pylori* infected dendritic cells. *European journal of immunology* 2013;**43**:2650-8.

34 Semper RP, Mejías-Luque R, Groß C, et al. *Helicobacter pylori*-induced IL-1ß secretion in innate immune cells is regulated by the NLRP3 inflammasome and requires the *cag* pathogenicity island. *J Immunol* 2014;**193**:3566-76.

35 Lu W, Hisatsune A, Koga T, et al. Cutting edge: enhanced pulmonary clearance of *Pseudomonas aeruginosa* by Muc1 knockout mice. *J Immunol* 2006;**176**:3890-4.

36 Ueno K, Koga T, Kato K, et al. MUC1 mucin is a negative regulator of Toll-like receptor signaling. *Am J Respir Cell Mol Biol* 2008;**38**:263-8.

37 Sheng YH, Triyana S, Wang R, et al. MUC1 and MUC13 differentially regulate epithelial inflammation in response to inflammatory and infectious stimuli. *Mucosal Immunol* 2013;**6**:557-68.

38 Bauernfeind FG, Horvath G, Stutz A, et al. Cutting edge: NF-κB activating pattern recognition and cytokine receptors license NLRP3 inflammasome activation by regulating NLRP3 expression. *J Immunol* 2009;**183**:787-91.

39 Guha M, Mackman N. LPS induction of gene expression in human monocytes. *Cell Signal* 2001;**13**:85-94.

40 Haneklaus M, Gerlic M, Kurowska-Stolarska M, et al. Cutting Edge: miR-223 and EBV miR-BART15 regulate the NLRP3 inflammasome and IL-1β production. *J Immunol* 2012;**189**:3795-9.

41 Horng T. Calcium signaling and mitochondrial destabilization in the triggering of the NLRP3 inflammasome. *Trends Immunol* 2014;**35**:253-61.

42 Ahmad R, Raina D, Trivedi V, et al. MUC1 oncoprotein activates the IκB kinase β complex and constitutive NF-κB signalling. *Nat Cell Biol* 2007;**9**:1419-27.

43 Crabtree JE, Ferrero RL, Kusters JG. The mouse colonizing *Helicobacter pylori* strain SS1 may lack a functional *cag* pathogenicity island. *Helicobacter* 2002;**7**:139-40.

44 Flannery S, Bowie AG. The interleukin-1 receptor-associated kinases: Critical regulators of innate immune signalling. *Biochem Pharmacol* 2010;**80**:1981-91.

45 Kato K, Lillehoj EP, Park YS, et al. Membrane-tethered MUC1 mucin is phosphorylated by epidermal growth factor receptor in airway epithelial cells and associates with TLR5 to inhibit recruitment of MyD88. *J Immunol* 2012;**188**:2014-22.

46 Hitzler I, Sayi A, Kohler E, et al. Caspase-1 has both proinflammatory and regulatory properties in *Helicobacter* infections, which are differentially mediated by its substrates IL-1β and IL-18. *J Immunol* 2012;**188**:3594-602.

47 Oertli M, Sundquist M, Hitzler I, et al. DC-derived IL-18 drives Treg differentiation, murine *Helicobacter pylori*-specific immune tolerance, and asthma protection. *J Clin Invest* 2012;**122**:1082-96.

48 Benoit BN, Kobayashi M, Kawakubo M, et al. Role of ASC in the mouse model of *Helicobacter pylori* infection. *J Histochem Cytochem* 2009;**57**:327-38.

49 Hmadcha A, Bedoya FJ, Sobrino F, et al. Methylation-dependent gene silencing induced by interleukin 1β via nitric oxide production. *J Exp Med* 1999;**190**:1595-604.

FIGURE LEGENDS

Figure 1: MUC1 protects against gastric dysplasia and death during chronic *H. pylori* infection in mice.

Wildtype and *Muc1*$^{-/-}$ mice were infected with *H. pylori* SS1 (n=8 uninfected and n=26 infected each). (A) Kaplan-Meier survival curve, considering mice that required euthanasia on ethical grounds as events and mice which did not exhibit clinical signs as censored. *H. pylori* infection was a significant cause of death in *Muc1*$^{-/-}$ mice (Mantel-Cox). (B) Blinded H&E stained gastric sections from wildtype (WT) and *Muc1*$^{-/-}$ mice that were left uninfected or infected for ≥8 months were assessed for inflammation. Graphs present individual mice (points) and group medians (horizontal bar). *H. pylori* infected *Muc1*$^{-/-}$ mice developed significantly more severe mononuclear cellular infiltrate and atrophy (*Mann-Whitney) and a significantly higher proportion developed atrophy and dysplasia ($^{\#}$Fisher's exact test) compared to infected wildtype mice. (C) A colony-forming assay was performed on half stomachs from wildtype and *Muc1*$^{-/-}$ mice that had been infected for ≥8 months. *Muc1*$^{-/-}$ mice had significantly reduced CFU compared to wildtype mice (ANOVA).

Figure 2: Representative gastric histopathology from mice with chronic *H. pylori* infection

(A) Uninfected, average and severe pathology observed in infected *Muc1*$^{-/-}$ mice. (B) Average pathology observed in infected wildtype mice is shown. 100 μM scale bars. Solid line indicates cystic dysplasia, shown in higher magnification in (C); dashed and dotted lines indicate "nuclear" dysplasia, shown in higher magnification in (D) (20 μM scale bars).

Figure 3: Increased pathology in *Muc1*$^{-/-}$ mice is associated with elevated gastric IL-1β.

Wildtype (WT) and *Muc1*$^{-/-}$ mice were infected with a single dose of *H. pylori* SS1 for 1, 2 (n=5-12) or 8+ months (as in Figure 1). Cytokines in gastric homogenates were quantified by ELISA. Age-matched negative controls were left uninfected (U) and analysed simultaneously with the infected mice. *Muc1*$^{-/-}$ stomachs had significantly elevated IL-1β compared to wildtype stomachs after two months and long-term infection (ANOVA). Data for 1-2 month infections were pooled from 2 separate experiments. Graphs present the median (horizontal bar), interquartile range (box) and 10th and 90th percentiles (bars).

Figure 4: Increased *Tff2* promoter methylation in *H. pylori*-infected *Muc1*$^{-/-}$ mice and in H^+K^+ATPase/hIL-1β transgenic mice.

(A) *Tff2* methylation sites. (B) qRT-PCR analysis of *Tff2* mRNA expression levels in stomach tissue from H^+K^+ATPase/hIL-1β transgenic (*IL-1β* Tg*)* mice and wildtype controls. *IL-1β* Tg mice expressed reduced *Tff2* consistent with increased gene methylation (Mann-Whitney) (C, D) Quantitative *Tff2* promoter methylation analysis in *IL-1*β Tg mice and wildtype controls. (C) Boxplot showing CpG methylation levels expressed as the ratio of total methylated/unmethylated DNA at four CpG dinucleotides in the *Tff2* promoter region. There was significantly increased *Tff2* promoter methylation in *IL-1β* Tg mice compared to wildtype mice (ANOVA). (D) Heatmap showing two-way hierarchical cluster analysis of the data presented in (C), annotation as described above. *IL-1β* Tg samples are identified within the heatmap by black shading in the key to the right. (E, F) Quantitative *Tff2* promoter methylation analysis in 8+ month *H. pylori* infected wildtype (WT) and *Muc1*$^{-/-}$ mice together with age-matched uninfected controls (as in Figure 1). (E) Box plot showing CpG methylation levels; infected *Muc1*$^{-/-}$ mice had significantly increased methylation compared to infected wildtype mice (ANOVA). (F) Heatmap showing two-way hierarchical cluster analysis of CpG methylation (columns) and stomach tissue samples (rows) of the data presented in (E). Differential methylation levels are colour coded; areas of low methylation (green), high methylation (red). *H. pylori* infected *Muc1*$^{-/-}$ samples are identified within the heatmap by black shading in the key to the right. (G) qRT-PCR analysis of *Tff2* mRNA levels in stomach tissue from 8+ month *H. pylori* infected wildtype (WT) and *Muc1*$^{-/-}$ mice together with controls. Both infected WT and *Muc1*$^{-/-}$ mice had significantly reduced *Tff2* levels compared to uninfected controls (ANOVA).

Figure 5: Increased pathology in *Muc1*$^{-/-}$ mice is dependent on MUC1-deficient hematopoietic cells.

(A) Recipient wildtype and *Muc1*$^{-/-}$ mice were irradiated and injected with bone marrow cells from either syngeneic or allogeneic donors. After 2 months reconstitution, chimaeric mice were infected with *H. pylori* SS1. Gastric inflammation was graded histologically and parietal cells quantitated (gland atrophy) 2 months post-infection. Only mice receiving *Muc1*$^{-/-}$ bone marrow developed significant atrophic gastritis (p values cf wildtype syngeneic control; Mann-Whitney). Graphs present individual mice (points) and group medians (horizontal bar). Representative photomicrographs with typical pathology are shown of (B) an infected *Muc1*$^{-/-}$ mouse reconstituted with wildtype bone marrow and (C) an infected wildtype mouse reconstituted with *Muc1*$^{-/-}$ bone marrow (100 μM scale bars).

Figure 6: *Muc1*$^{-/-}$ mice have increased gastric recruitment of specific cell types after infection.

Wildtype (WT) and *Muc1*$^{-/-}$ mice (n=5) were infected with a single dose of *H. pylori* SS1 for 2 months or left uninfected. Cells were isolated from stomachs and analysed by flow cytometry. (A) Gating strategy used to identify particular immune cells. (B) Numbers of immune cell types in the gastric compartment. Infected *Muc1*$^{-/-}$ mice had significantly increased numbers of dendritic cells and P2 monocyte/macrophages compared to wildtype mice (ANOVA). Graphs present the median (horizontal bar), interquartile range (box) and 10th and 90th percentiles (bars).

Figure 7: MUC1 regulates the inflammasome response to *H. pylori* infection.

(A) Wildtype macrophages (n=7) and dendritic cells (n=8) were stimulated overnight with *H. pylori* lysate or live *H. pylori* with or without glyburide. Live *H. pylori* and to a lesser extent *H. pylori* lysate induced IL-1β production in a manner that could be inhibited by glyburide (*ANOVA cf media; #ANOVA cf *H. pylori* alone). (B) IL-1β levels in supernatants of wildtype (WT) and *Muc1*$^{-/-}$ macrophages or dendritic cells (n=6) cultured overnight with *H. pylori* lysate (ELISA). (C) IL-18 levels in supernatants from WT and *Muc1*$^{-/-}$ macrophages (ELISA). *Muc1*$^{-/-}$ cells secreted significantly more IL-1β and IL-18 (ANOVA). (D) *Muc1*$^{-/-}$ and *Casp1*$^{-/-}$ mice, interbred to produce F3 *Muc1*$^{-/-}$*Casp1*$^{-/-}$ mice and matched controls, were infected with *H. pylori* SS1 (n=11 wildtype, n=8 *Muc1*$^{-/-}$ and n=6 *Muc1*$^{-/-}$*Casp1*$^{-/-}$). Age matched littermates were left uninfected as controls (n=6 wildtype, n=7 *Muc1*$^{-/-}$ and n=2 *Muc1*$^{-/-}$*Casp1*$^{-/-}$). Gastric inflammation was assessed histologically two months post-infection. *Muc1*$^{-/-}$ mice but not *Muc1*$^{-/-}$*Casp1*$^{-/-}$ mice developed a significant atrophic gastritis (p values cf infected wildtype; Mann-Whitney). Graphs present individual mice (points) and group medians (horizontal bar). (E) Representative photomicrographs showing typical pathology from infected *Muc1*$^{-/-}$ and *Muc1*$^{-/-}$*Casp1*$^{-/-}$ mice (100 μM scale bars).

Figure 8: MUC1 regulation of NLRP3 expression and NF-κB pathway activation via inhibition of IRAK4 phosphorylation

(A) Stomachs from *Muc1*$^{-/-}$ mice infected with *H. pylori* for 2 months (n=6) had elevated *Nlrp3* expression (by qRT-PCR) relative to infected wildtype stomachs (ANOVA). (B) NLRP3 protein induction in LPS or *H. pylori* lysate stimulated macrophages was examined by western blot. A representative blot (2 independent experiments for LPS) is shown with densitometry values after 3 hours stimulation (n=4 for LPS; n=3 for *H. pylori* lysate). *Muc1*$^{-/-}$ macrophages expressed significantly higher levels of NLRP3 3 hours after stimulation (ANOVA). (C) Relative mRNA expression of *Nlrp3* in macrophages pulsed with BAY 11-7082 for 45 min prior to stimulation with LPS or *H. pylori* lysate (n=5). *Muc1*$^{-/-}$ cells had significantly higher levels of *Nlrp3* expression compared to wildtype cells after 3 hours stimulation (ANOVA). BAY 11-7082 inhibited upregulation of *Nlrp3*. Graphs present the median (horizontal bar), interquartile range (box) and 10th and 90th percentiles (bars). (D, E) Activation of NF-κB following stimulation with LPS or *H. pylori* lysate was assessed by western blotting of phosphorylated and total forms of p65 and IKKs. Representative blots are shown with densitometry values from 6 (LPS) or 5 (*H. pylori* lysate) separate experiments (mean and SEM). Stimulated *Muc1*$^{-/-}$ cells had increased phosphorylation of both p65 and IKKα/β compared to wildtype cells (ANOVA). (F, G) Activation of IRAK4 was assessed by western blotting of phosphorylated and total forms. Representative blots are shown with densitometry values from 3 (LPS) and 6 (*H. pylori* lysate) separate experiments (mean and SEM). *Muc1*$^{-/-}$ cells had increased phosphorylation of IRAK4 compared to wildtype cells following stimulation with either (F) LPS or (G) *H. pylori* (ANOVA). (H) Relative *Nlrp3* expression in macrophages pulsed with IRAK1/4 inhibitor I for 30 min prior to *H. pylori* lysate stimulation for 3 hours (n=5). IRAK1/4 inhibitor I inhibited upregulation of *Nlrp3*. Graph presents the median (horizontal bar), interquartile range (box) and 10th and 90th percentiles (bars).

Figure 9: Atrophic gastritis in *Muc1*$^{-/-}$ mice is NLRP3 dependent.

Muc1$^{-/-}$ and *Nlrp3*$^{-/-}$ mice were interbred to produce F3 *Muc1*$^{-/-}$*Nlrp3*$^{-/-}$ mice and age-matched littermate controls. Mice were infected with *H. pylori* SS1 for two months or left uninfected. (A) Macrophages from uninfected mice (n=6) were stimulated overnight with *H. pylori* lysate and IL-1β levels measured by ELISA. *Muc1*$^{-/-}$ but not *Muc1*$^{-/-}$*Nlrp3*$^{-/-}$ macrophages produced increased IL-1β compared to wildtype macrophages. (B) Infected *Muc1*$^{-/-}$ but not *Muc1*$^{-/-}$ *Nlrp3*$^{-/-}$ mice (n=7) had significantly elevated gastric IL-1β and IL-18 (ELISA; ANOVA). (C) Gastric inflammation was assessed histologically. Infected *Muc1*$^{-/-}$ but not *Muc1*$^{-/-}$*Nlrp3*$^{-/-}$ mice developed a significant atrophic gastritis (p values cf infected wildtype; Mann-Whitney). Graphs present individual mice (points) and group medians (horizontal bar). (D) Representative photomicrographs showing typical pathology from infected *Muc1*$^{-/-}$ and *Muc1*$^{-/-}$*Nlrp3*$^{-/-}$ mice (100 μM scale bars).

Figure 1

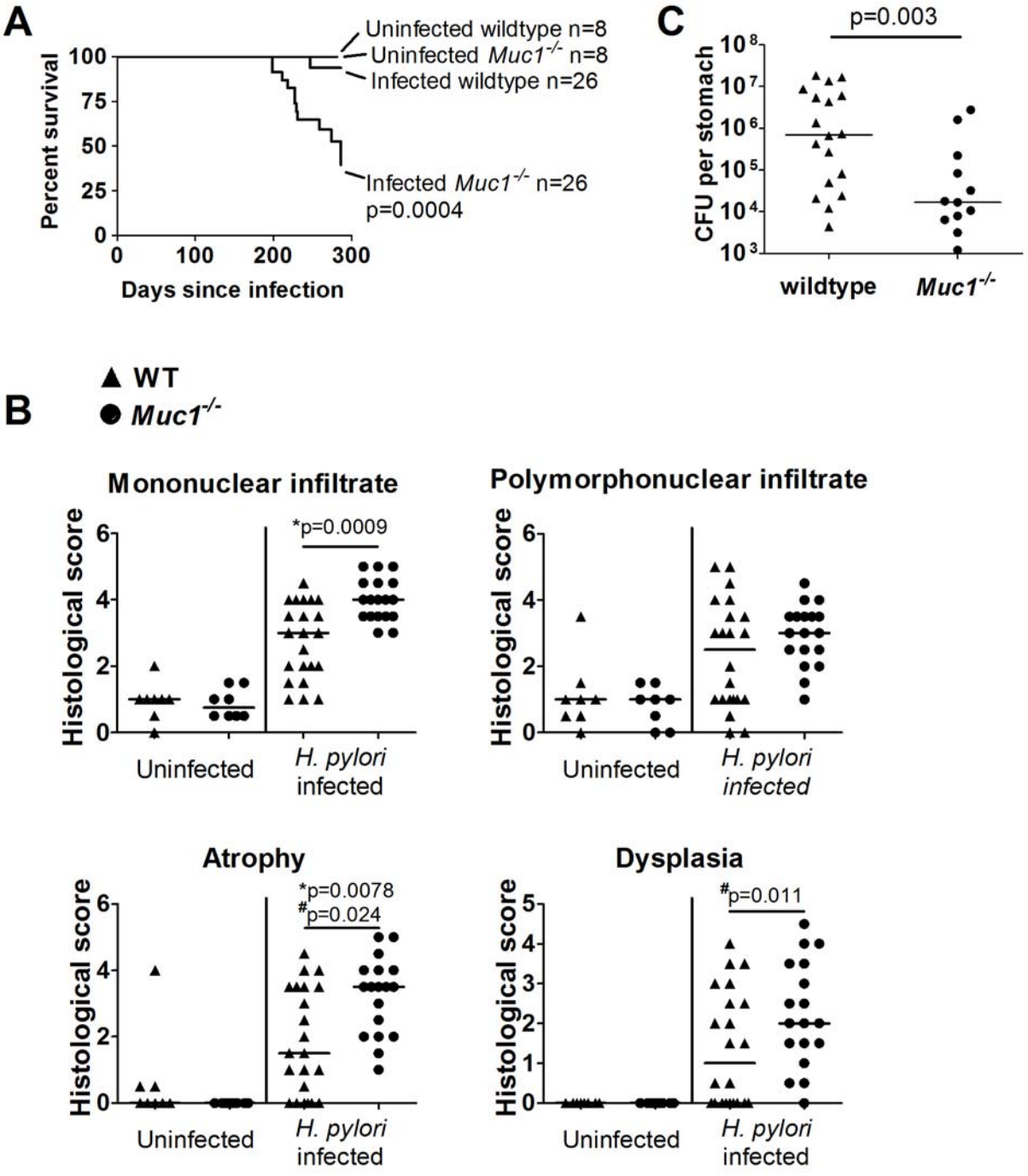
A
Uninfected wildtype n=8
Uninfected Muc1-/- n=8
Infected wildtype n=26
Infected Muc1-/- n=26
p=0.0004
Percent survival
Days since infection
C
p=0.003
CFU per stomach
wildtype
Muc1-/-
B
WT
Muc1-/-
Mononuclear infiltrate
*p=0.0009
Histological score
Uninfected
H. pylori infected
Polymorphonuclear infiltrate
Atrophy
*p=0.0078
#p=0.024
Dysplasia
#p=0.011

Figure 2

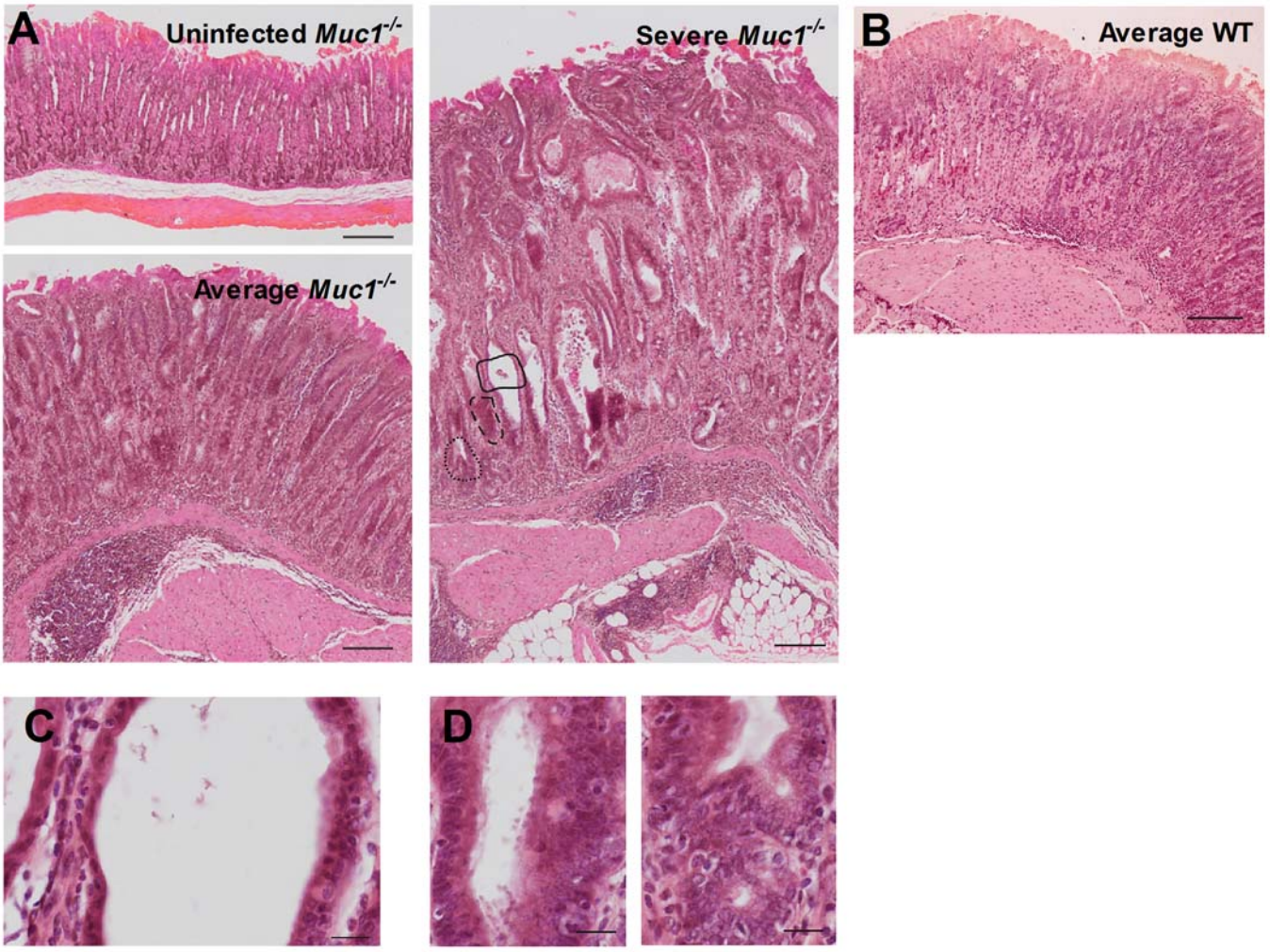

Figure 3

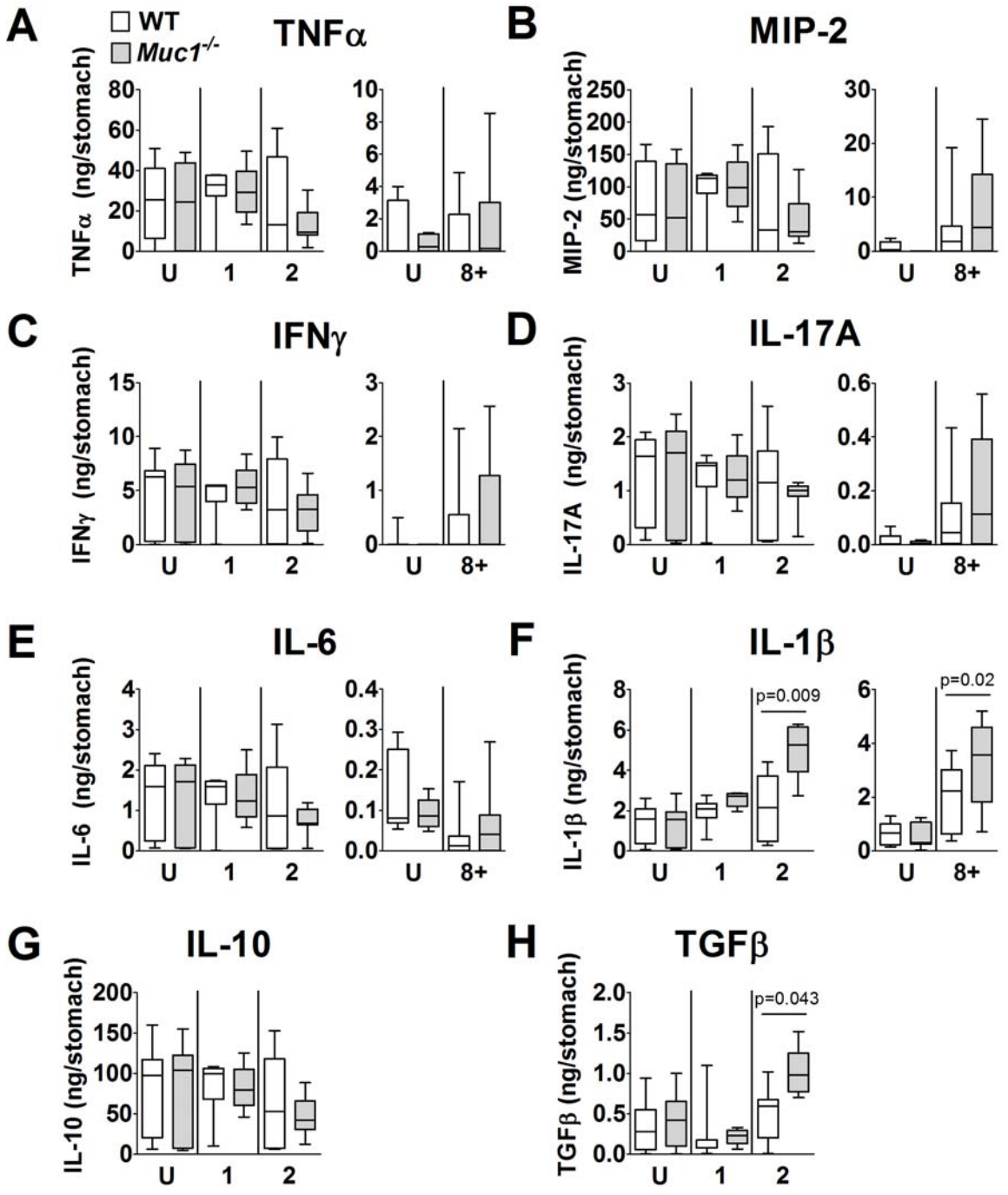
A
WT
Muc1-/-
TNFα
TNFα (ng/stomach)
B
MIP-2
MIP-2 (ng/stomach)
C
IFNγ
IFNγ (ng/stomach)
D
IL-17A
IL-17A (ng/stomach)
E
IL-6
IL-6 (ng/stomach)
F
IL-1β
IL-1β (ng/stomach)
p=0.009
p=0.02
G
IL-10
IL-10 (ng/stomach)
H
TGFβ
TGFβ (ng/stomach)
p=0.043
U
1
2
8+

Figure 4

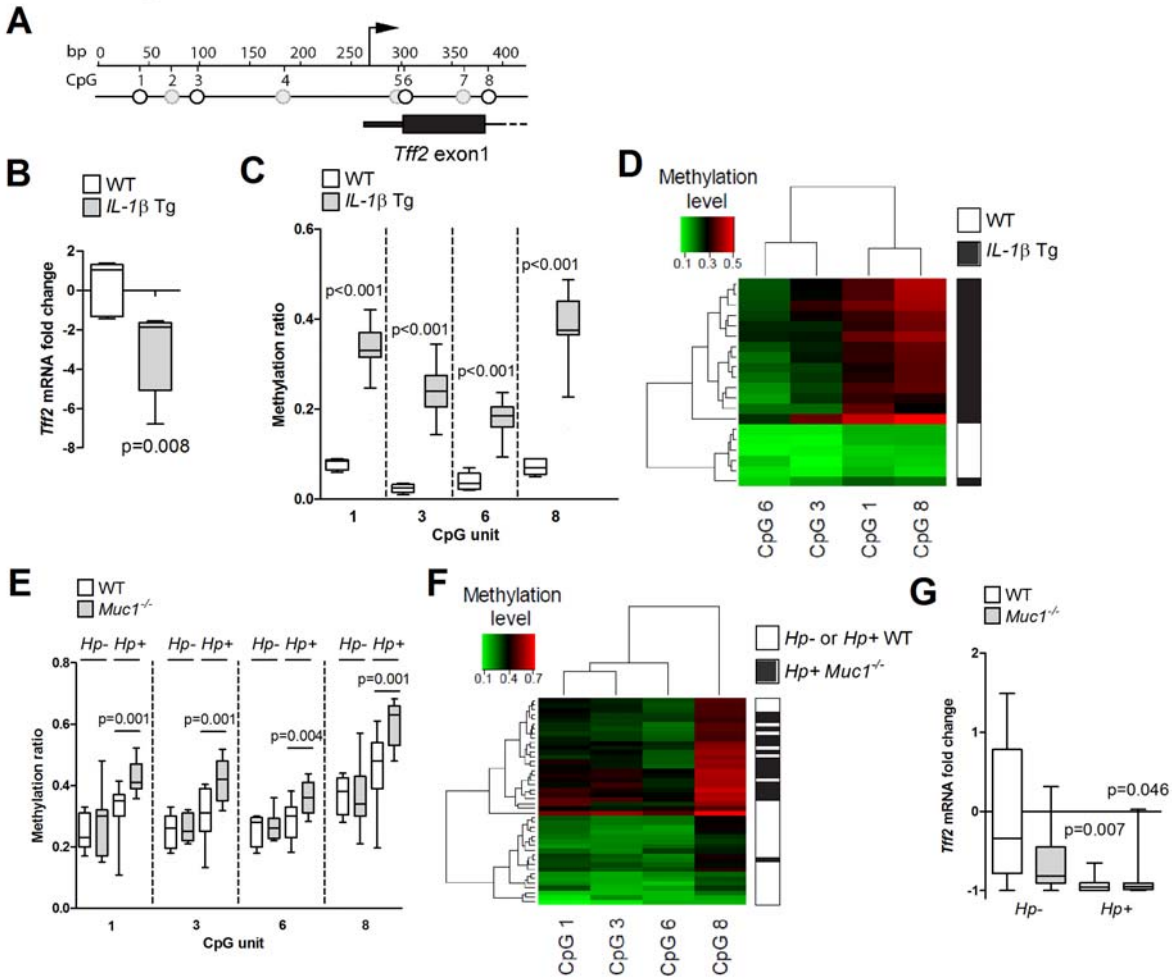
A
bp 0 50 100 150 200 250 300 350 400
CpG 1 2 3 4 5 6 7 8
Tff2 exon1
B
WT
IL-1β Tg
Tff2 mRNA fold change
p=0.008
C
WT
IL-1β Tg
Methylation ratio
p<0.001
p<0.001
p<0.001
p<0.001
CpG unit
D
Methylation level
0.1 0.3 0.5
WT
IL-1β Tg
CpG 6
CpG 3
CpG 1
CpG 8
E
WT
Muc1-/-
Hp- Hp+
Methylation ratio
p=0.001
p=0.001
p=0.004
p=0.001
CpG unit
F
Methylation level
0.1 0.4 0.7
Hp- or Hp+ WT
Hp+ Muc1-/-
CpG 1
CpG 3
CpG 6
CpG 8
G
WT
Muc1-/-
Tff2 mRNA fold change
p=0.046
p=0.007
Hp-
Hp+

Figure 5

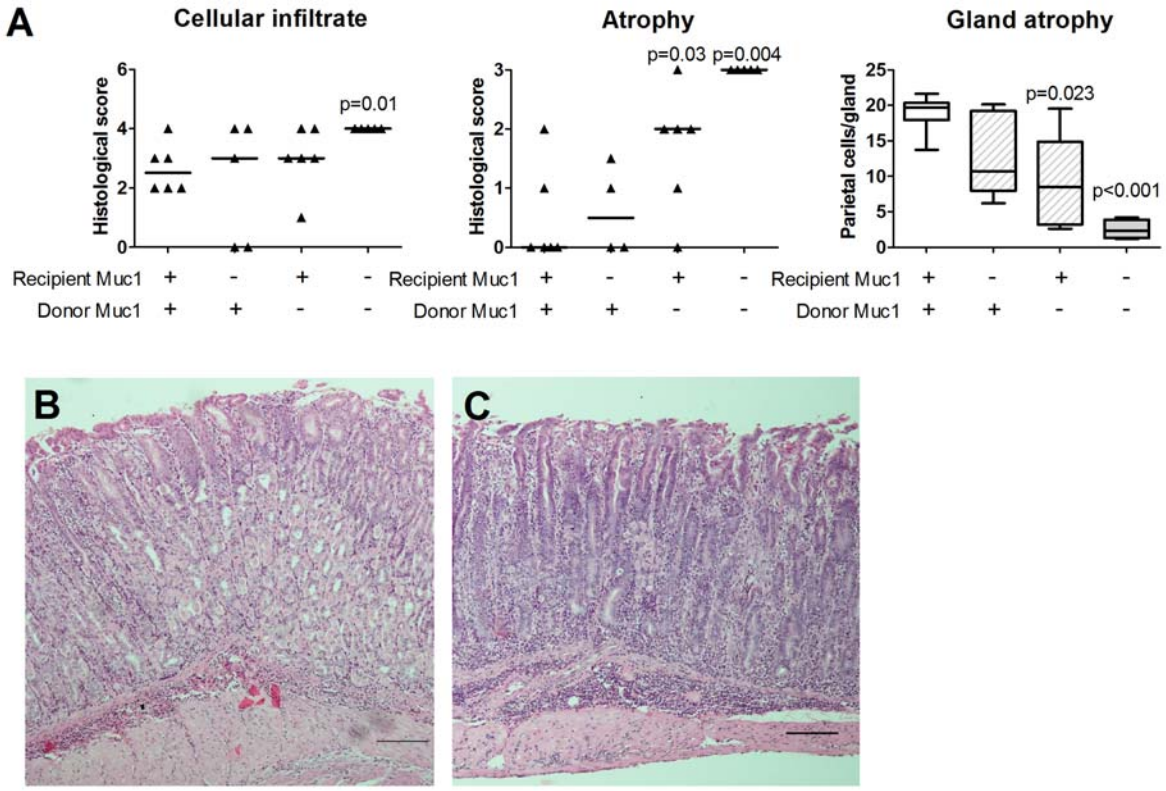
A
Cellular infiltrate
Histological score
p=0.01
Recipient Muc1 + - + -
Donor Muc1 + + - -
Atrophy
Histological score
p=0.03 p=0.004
Recipient Muc1 + - + -
Donor Muc1 + + - -
Gland atrophy
Parietal cells/gland
p=0.023
p<0.001
Recipient Muc1 + - + -
Donor Muc1 + + - -
B
C

Figure 6

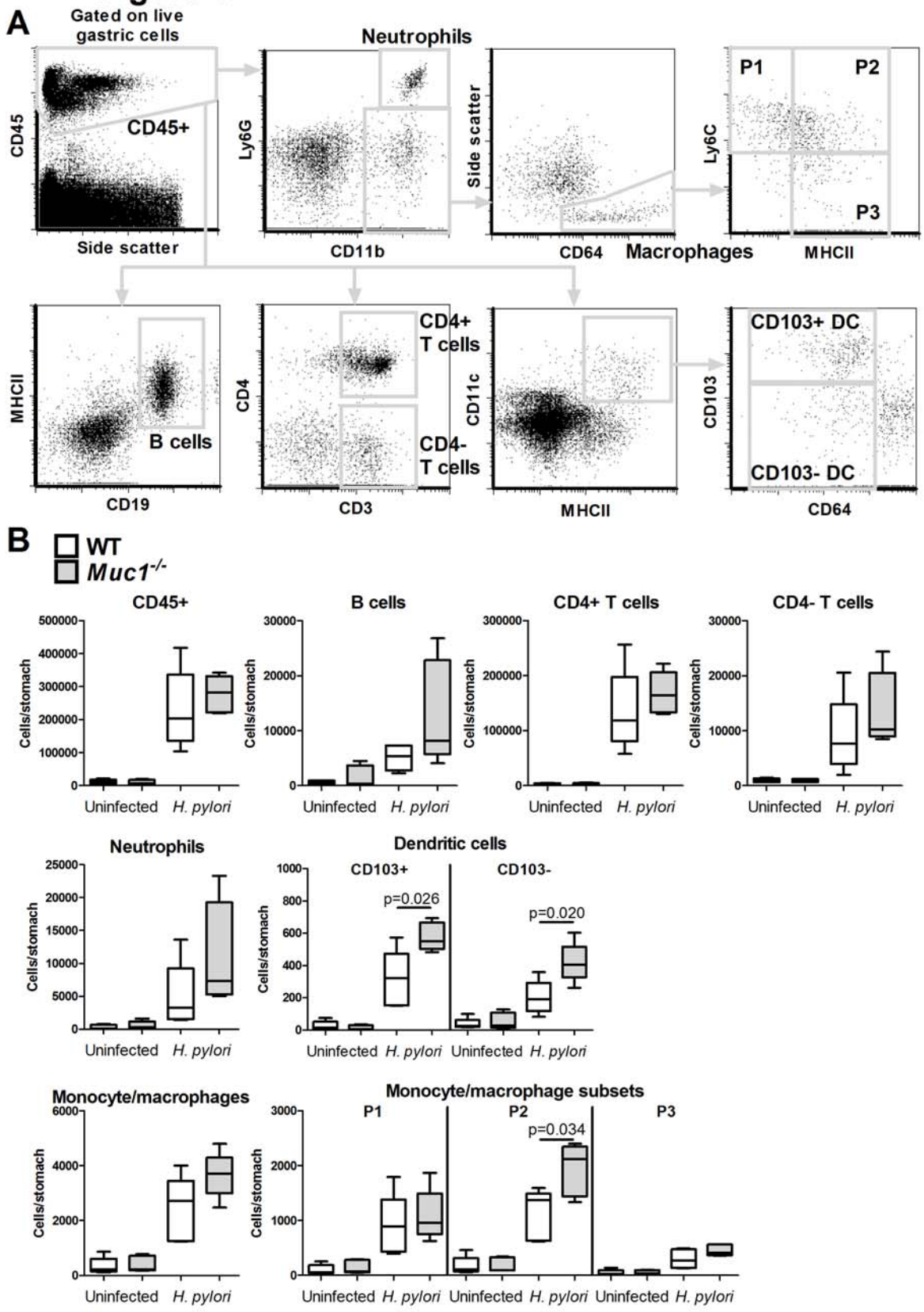
A
Gated on live gastric cells
CD45
CD45+
Side scatter
Neutrophils
Ly6G
CD11b
Side scatter
CD64
Macrophages
P1
P2
P3
Ly6C
MHCII
MHCII
B cells
CD19
CD4
CD4+ T cells
CD4- T cells
CD3
CD11c
MHCII
CD103
CD103+ DC
CD103- DC
CD64
B
WT
Muc1-/-
CD45+
B cells
CD4+ T cells
CD4- T cells
Cells/stomach
Uninfected
H. pylori
Neutrophils
Dendritic cells
CD103+
CD103-
p=0.026
p=0.020
Monocyte/macrophages
Monocyte/macrophage subsets
P1
P2
P3
p=0.034

Figure 7

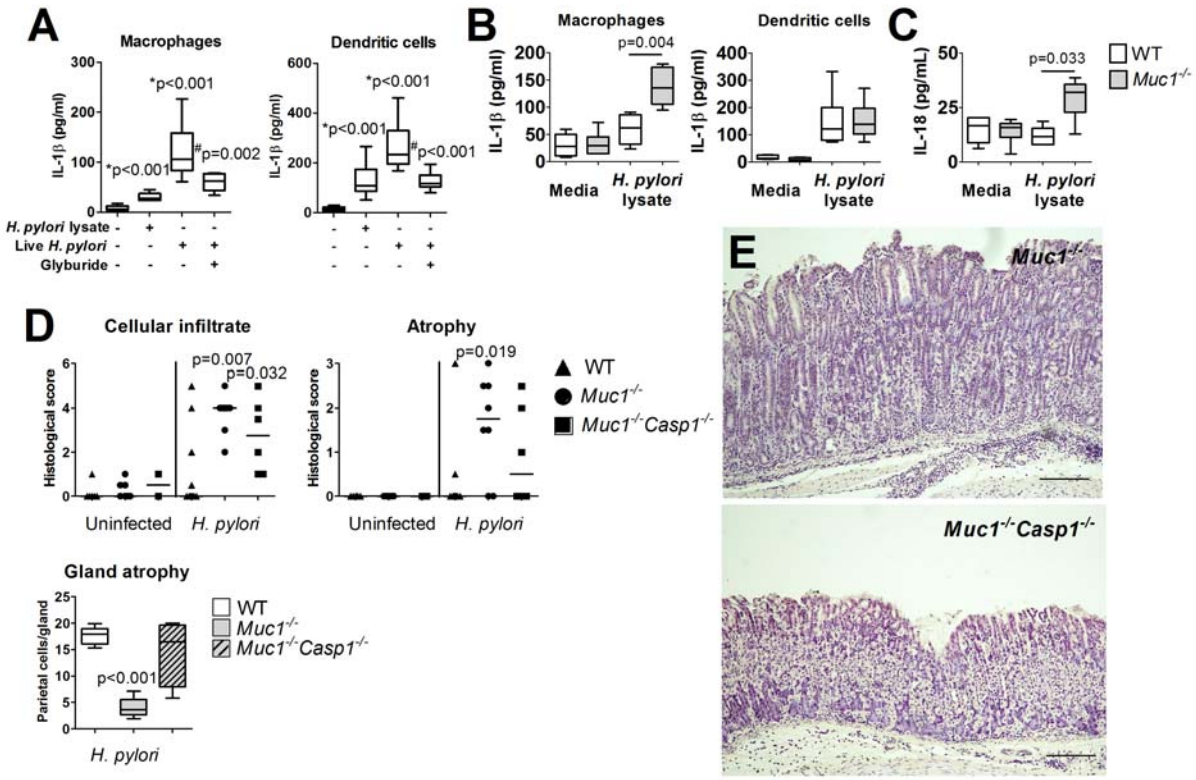
A
Macrophages
Dendritic cells
IL-1β (pg/ml)
*p<0.001
#p=0.002
H. pylori lysate
Live H. pylori
Glyburide
B
Macrophages
Dendritic cells
p=0.004
Media
H. pylori lysate
C
IL-18 (pg/mL)
p=0.033
WT
Muc1-/-
D
Cellular infiltrate
Atrophy
Histological score
p=0.007
p=0.032
p=0.019
Uninfected
H. pylori
WT
Muc1-/-
Muc1-/-Casp1-/-
Gland atrophy
Parietal cells/gland
p<0.001
E
Muc1-/-
Muc1-/-Casp1-/-

Figure 8

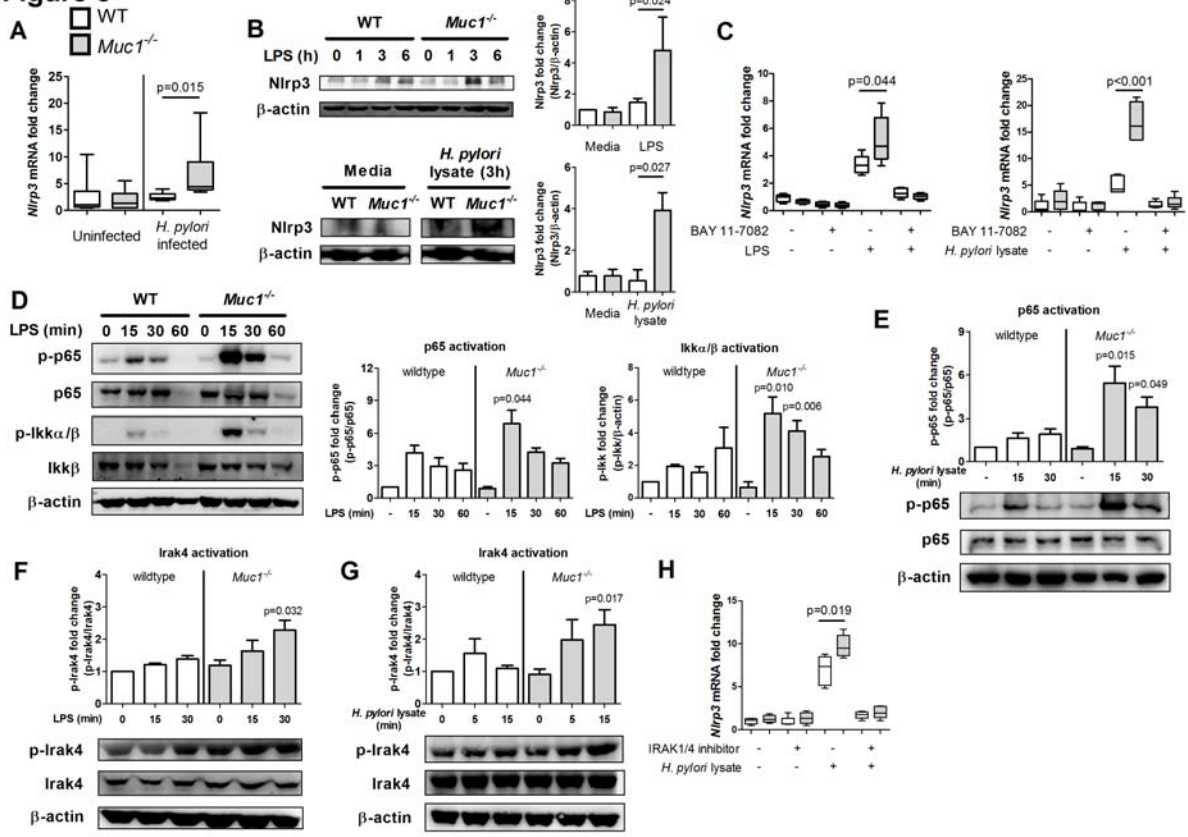
A
WT
Muc1-/-
Nlrp3 mRNA fold change
p=0.015
Uninfected
H. pylori infected
B
WT
Muc1-/-
LPS (h) 0 1 3 6 0 1 3 6
Nlrp3
β-actin
Media
H. pylori lysate (3h)
WT Muc1-/- WT Muc1-/-
Nlrp3
β-actin
Nlrp3 fold change (Nlrp3/β-actin)
p=0.024
Media LPS
p=0.027
Media H. pylori lysate
C
Nlrp3 mRNA fold change
p=0.044
BAY 11-7082 - + - +
LPS - - + +
p<0.001
BAY 11-7082 - + - +
H. pylori lysate - - + +
D
WT
Muc1-/-
LPS (min) 0 15 30 60 0 15 30 60
p-p65
p65
p-Ikkα/β
Ikkβ
β-actin
p65 activation
wildtype
Muc1-/-
p-p65 fold change (p-p65/p65)
p=0.044
LPS (min) - 15 30 60 - 15 30 60
Ikkα/β activation
wildtype
Muc1-/-
p-Ikk fold change (p-Ikk/β-actin)
p=0.010
p=0.006
LPS (min) - 15 30 60 - 15 30 60
E
p65 activation
wildtype
Muc1-/-
p-p65 fold change (p-p65/p65)
p=0.015
p=0.049
H. pylori lysate (min) - 15 30 - 15 30
p-p65
p65
β-actin
F
Irak4 activation
wildtype
Muc1-/-
p-Irak4 fold change (p-Irak4/Irak4)
p=0.032
LPS (min) 0 15 30 0 15 30
p-Irak4
Irak4
β-actin
G
Irak4 activation
wildtype
Muc1-/-
p-Irak4 fold change (p-Irak4/Irak4)
p=0.017
H. pylori lysate (min) 0 5 15 0 5 15
p-Irak4
Irak4
β-actin
H
Nlrp3 mRNA fold change
p=0.019
IRAK1/4 inhibitor - + - +
H. pylori lysate - - + +

Figure 9

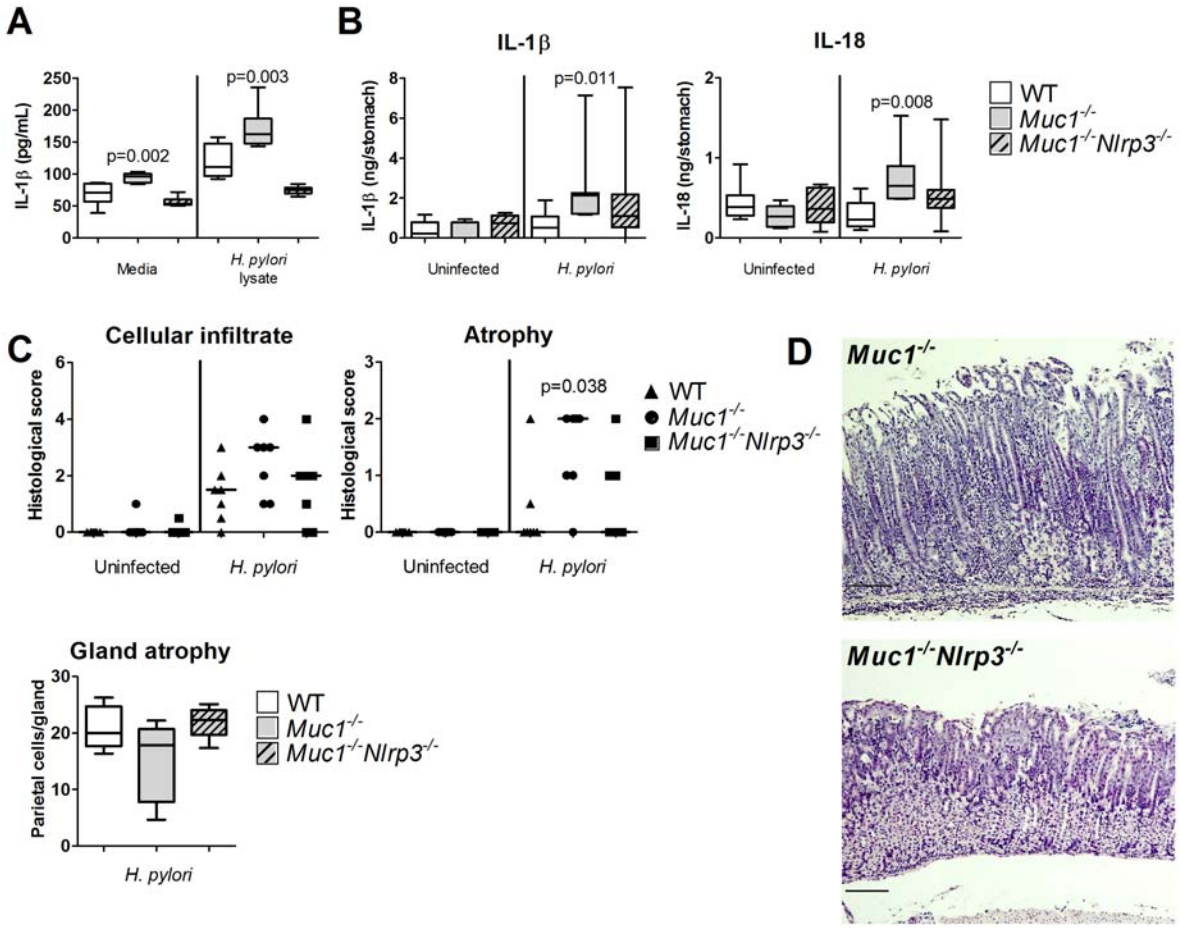
A
IL-1β (pg/mL)
p=0.002
p=0.003
Media
H. pylori lysate
B
IL-1β
IL-18
IL-1β (ng/stomach)
IL-18 (ng/stomach)
p=0.011
p=0.008
Uninfected
H. pylori
WT
Muc1-/-
Muc1-/-Nlrp3-/-
C
Cellular infiltrate
Atrophy
Histological score
p=0.038
Gland atrophy
Parietal cells/gland
D
Muc1-/-
Muc1-/-Nlrp3-/-

Author/s:
Ng, GZ; Menheniott, TR; Every, AL; Stent, A; Judd, LM; Chionh, YT; Dhar, P; Komen, JC; Giraud, AS; Wang, TC; McGuckin, MA; Sutton, P

Title:
The MUC1 mucin protects against Helicobacter pylori pathogenesis in mice by regulation of the NLRP3 inflammasome

Date:
2016-07-01

Citation:
Ng, G. Z., Menheniott, T. R., Every, A. L., Stent, A., Judd, L. M., Chionh, Y. T., Dhar, P., Komen, J. C., Giraud, A. S., Wang, T. C., McGuckin, M. A. & Sutton, P. (2016). The MUC1 mucin protects against Helicobacter pylori pathogenesis in mice by regulation of the NLRP3 inflammasome. GUT, 65 (7), pp.1087-U211. https://doi.org/10.1136/gutjnl-2014-307175.